Simulation of continuous terahertz wave transient state thermal effects on static water*

Lü Ying-Jin(吕英进)[a)b)], Xu De-Gang(徐德刚)[a)b)†], Liu Peng-Xiang(刘鹏翔)[a)b)], Lü Da(吕 达)[a)b)], Wen Qi-Ye(文岐业)[c)], Zhang Huai-Wu(张怀武)[c)], and Yao Jian-Quan(姚建铨)[a)b)]

[a)] *College of Precision Instruments and Opto-electronics Engineering, Tianjin University, Tianjin* 300072, *China*

[b)] *Key Laboratory of Opto-electronics Information Technology (Tianjin University), Ministry of Education, Tianjin* 300072, *China*

[c)] *State Key Laboratory of Electronic Films and Integrated Devices, University of Electronic Science and Technology of China, Chengdu* 610054, *China*

(Received 31 March 2011; revised manuscript received 18 April 2011)

We report a numerical simulation of continuous terahertz beam induced transient thermal effects on static water. The terahertz wave used in this paper has a Gaussian beam profile. Based on the transient heat conduction equation, the finite element method (FEM) is utilized to calculate the temperature distribution. The simulation results show the dynamic process of temperature change in water during terahertz irradiation. After about 300 s, the temperature reaches a steady state with a water layer thickness of 5 mm and a beam radius of 0.25 mm. The highest temperature increase is 7 K/mW approximately. This work motivates further study on the interaction between terahertz wave and bio-tissue, which has a high water content.

Keywords: terahertz, transient thermal effect, finite element method

PACS: 42.62.–b, 02.70.Dh, 44.10.+i **DOI:** 10.1088/1674-1056/20/10/104205

1. Introduction

Applications of terahertz (THz) technology have developed a great deal in the areas of package inspection,[1] bio-tissue imaging,[2] drug inspection,[3] security monitor,[4] communication,[5] water concentration measurement,[6] etc. The energies of THz photons are relatively lower than X-rays and safer for bio-tissue. However, this technology is not perfect. As bio-tissue has a high water content and because water can strongly absorb the THz wave, an obvious thermal effect may be induced in a biological body. In some experiments, it has been found that unusual behaviours occur under a certain THz irradiation, e.g. unconventional behaviour of male mice,[7] abnormal DNA dynamics DNA,[8] and infringement of neuron cellular membranes.[9] Recently, Torben *et al.*[10] reported a model of THz heating in water. Their paper was the only paper dealing with this subject until now. The increase in temperature can cause instability in some parameters during the THz application. With a beam spot of 0.5 mm, the temperature increased 1.8 K/mW. However, they only discussed the temperature change in a steady state. In addition, it is unrealistic to take the beam profile to be uniform.

The temperature distribution in a transient state is very important. During different THz applications, the irradiation times are different. It is necessary to know the time to reach a steady state and the dynamic process of temperature change, so that we can pay more attention to those significant thermal effects at a certain time. In addition, the Gaussian beam profile should be taken into consideration because it is more practical. The thermal effect can also be more obvious than the uniform beam profile because the power density is higher in the centre.

In this paper, by using Comsol software, we simulate the dynamic process of temperature rising with time in static water under THz irradiation. The THz wave has a Gaussian beam profile. From the simulation results, we find that the thickness of the water layer has an obvious influence on the time that is needed to arrive at a steady state, but the effects of the initial temperature of water and the source factors (beam radius, power, frequency) are small. It takes about 300 s for the temperature to reach a steady state when the water layer thickness is 5 mm and the

*Project supported by the National Basic Research Program of China (Grant Nos. 2007CB310403 and 2007CB310407) and the National Natural Science Foundation of China (Grant No. 60801017).

†Corresponding author. E-mail: xudegang@tju.edu.cn

© 2011 Chinese Physical Society and IOP Publishing Ltd

beam radius is 0.25 mm. The maximum temperature rise is 7 K/mW.

2. Method

The conventional THz-TDS causes little temperature change and it can be negligible.[10] We mainly focus on the thermal effect caused by a continuous THz wave. The absorption coefficient of water for a THz wave is relatively large. The typical value is of the order of 10^2 cm^{-1}–10^3 cm^{-1}. According to Lambert–Beer law, the transmission of a THz beam through a 1-mm-thick water layer is about zero, see Eq. (1) below

$$T = \frac{I}{I_0} = \mathrm{e}^{-\alpha d} \approx 0, \tag{1}$$

where I_0 and I are the intensities of the incident beam and the transmitted beam, respectively, and d is the penetration depth. So we consider that the incident power is completely absorbed by the water. At the water–air interface, the reflective rate is about 13% for 1 THz.[10] So there is a small difference between the incident power and the transmitted power. In this paper, we mainly investigate the transmitted power.

We choose a cylindrical water layer with thickness d and radius b as the model. The THz beam with radius a transfers through the centre of the circle point on the top surface (Fig. 1).

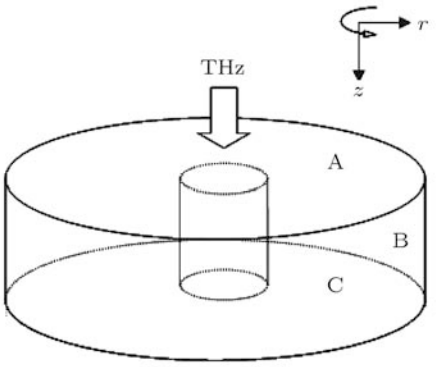


Fig. 1. Geometry of the water layer in the cylinder coordinate system.

The classical transient heat conduction equation is used in our simulation and it reads

$$\rho c \frac{\partial T}{\partial t} = \nabla(k(T)\nabla T) + Q(r, z), \tag{2}$$

where ρ is the water density; c is the water specific heat; T is the temperature distribution function of r, z, and t; k is the thermal conductivity of water; $Q(r, z)$ is the dissipated power density at the point (r, z), which can be determined by[11]

$$Q(r, z) = \frac{2P\alpha}{\pi a^2}(1 - \mathrm{e}^{-\alpha d})^{-1} \exp\left(-\frac{2r^2}{a^2}\right) \cdot \mathrm{e}^{-\alpha z}, \tag{3}$$

where P is the total power dissipated in the water and α is the absorption coefficient.

Values for the parameter thermal conductivity k and absorption coefficient α need not to be discussed.[10,12–14] For the calculation of the heat equation, we still need to set appropriate boundary conditions. A significant temperature change occurs mainly on the top surface,[10] it is reasonable to assume that the heat loss to the air is negligible. We take the surface A as being heat insolated. On the surface C, temperature increase caused by the laser is relatively small. So we consider the heat loss to be equal to the heat received, thus the temperature is kept constant. The side surface B is far from the source area, so we consider the temperature to be constant (Table 1).

Table 1. Definitions of boundary conditions.

Surface A: $z = 0$	$\partial T/\partial z = 0$
Surface B: $r = b$	$T = T_0$
Surface C: $z = d$	$T = T_0$

3. Simulation

We utilize Comsol software to perform the finite element method. The other parameters for the simulation are listed in Table 2.

Table 2. Initial values for the simulation.

Initial temperature/K	T_0=298.15
Frequency/THz	$f = 1$
Dissipated power/mW	$P = 1$
Beam radius/mm	$a = 0.25$
Water layer thickness/mm	$d = 5$
Water layer radius/mm	$b = 30$

In many cases, the medium is a slice which has a relatively small thickness. In our model, we set the thickness $d = 5$ mm and compare the temperatures between layers of different thickness. The thickness value is big enough to make the THz wave interact with the medium. In Fig. 2, we investigate the processes of temperature change at different points on the z axis ($r = 0$). It is clearly seen that the temperatures at different depths increase fast in the first 100 s, owing to the large slope. After about 300 s, the temperature trends to be constant. It is also proved that for Gaussian beam profile, the increment of steady state

temperature is higher than that of the uniform beam profile (~ 1.8 K).[10]

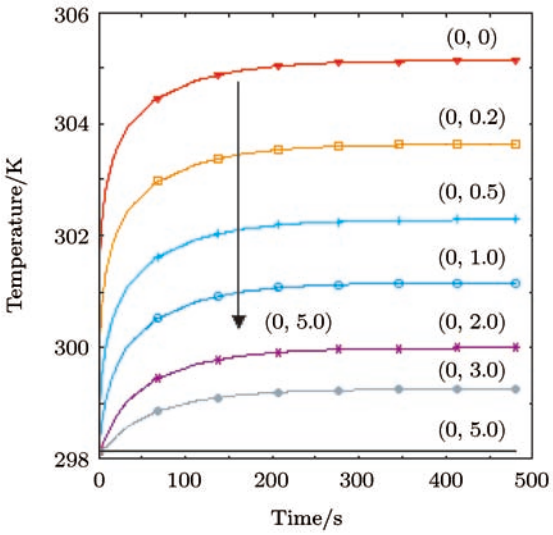


Fig. 2. Relationship between temperature and time to reach a steady state in different depths.

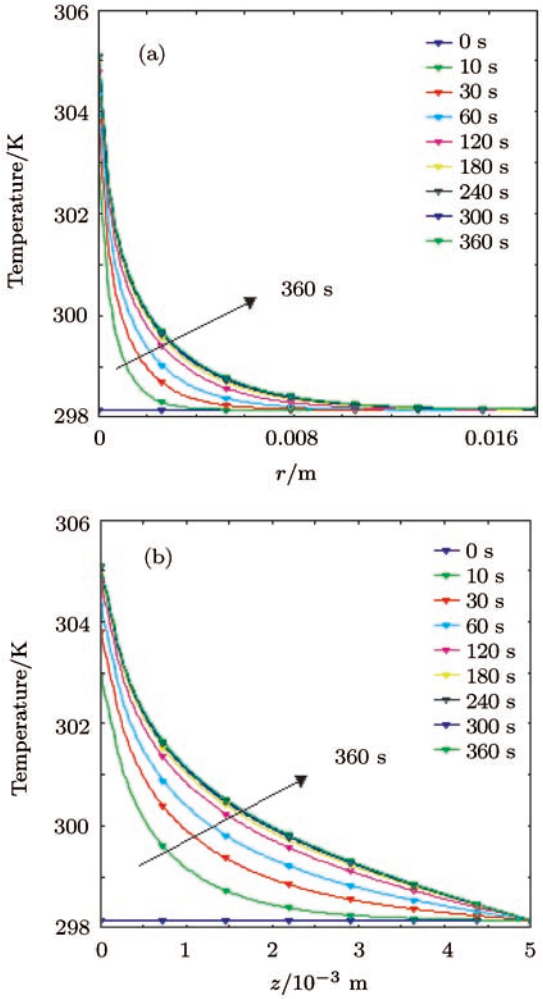


Fig. 3. Temperature versus time for (a) $z = 0$ along the r coordinate and (b) $r = 0$ along the z coordinate.

The processes of temperature increase on the top surface ($z = 0$) and in different depths ($r = 0$) are shown in Fig. 3. The exponential attenuation profiles along the r direction and the penetration depth verify the theory very well. All the lines overlap after about 300 s under the THz irradiation and the temperature reaches a steady state.

We are still concerned with the area that has a remarkable temperature increase. On the radial coordinate, we choose three different points $r = a$, $r = 2a$, and $r = 4a$. The temperature distributions along the z axis are shown in Fig. 4. When $z > 2.5$ mm, the temperature trends to be the same after 300 s at different points along the r axis, owing to the limited penetration depth of the THz beam in water. In Fig. 3(a), in the radial direction ($z = 0$), the maximum temperature increase is about 44% at $r = 4a$ (3.05 K) relative to $r = 0$ (6.96 K).

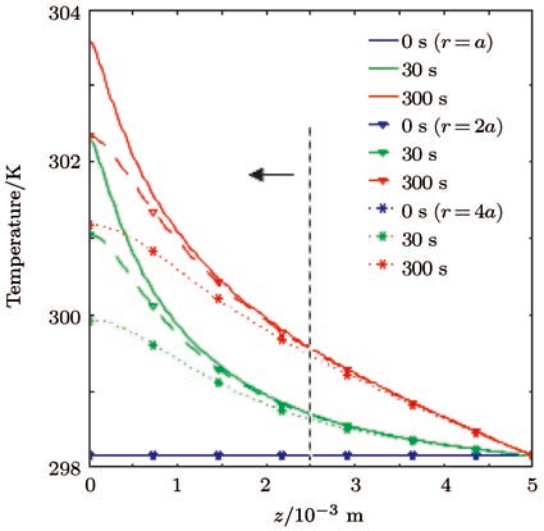


Fig. 4. Relationships between temperature and penetration depth with different radii on the top surface.

The calculations of water layer with different thicknesses and initial temperatures are shown in Fig. 5 and Fig. 6, respectively. The heating time to reach stability becomes shorter for thin layers. For $d = 1$ mm, the heating time is just about 25 s while for $d = 5$ mm, it is 300 s. As the thickness rises, the maximum temperature increases. It is easy to understand because more water absorbs more energy and needs more time. If the layer is too thin, the heat lost from the bottom surface is larger and the thermal equilibrium is easier to reach. However, the times expended in reaching a steady state for different initial temperatures of water are almost the same.

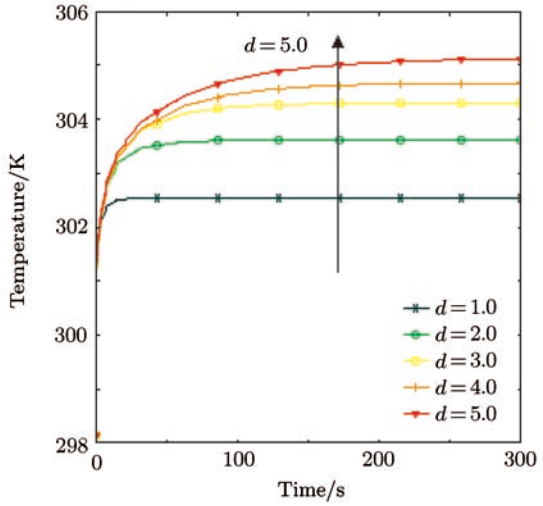


Fig. 5. Relationships between temperature and time for different thicknesses of water layer.

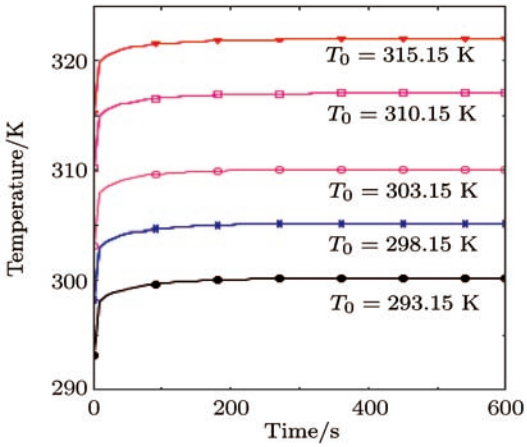


Fig. 6. Relationships between temperature and time for different initial temperatures of water layer.

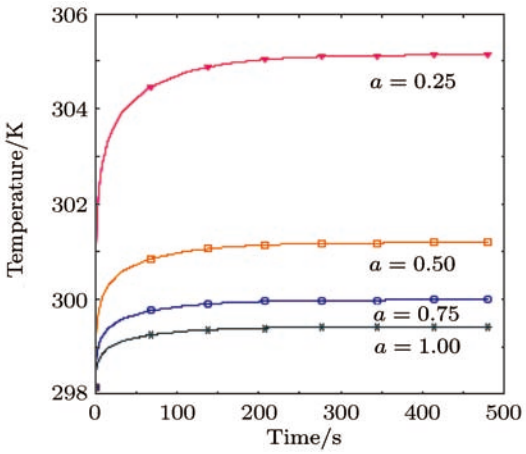


Fig. 7. Relationships between temperature and time with a THz wave of different beam radii.

In Figs. 7–9, we analyse the influence of the source factors: the beam radius, the power and the frequency. For different beam radii, powers and frequencies, the time expended in reaching a steady state is almost the same. As the beam radius increases, the power density decreases and the thermal effect becomes weak. The temperature increment is proportional to the power and the maximum value is 7 K/mW approximately. We can restrict the thermal effect by reducing power and frequency.

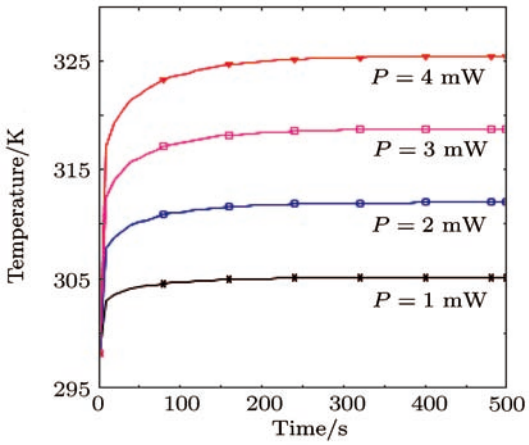


Fig. 8. Relationships between temperature and time for THz waves with different powers.

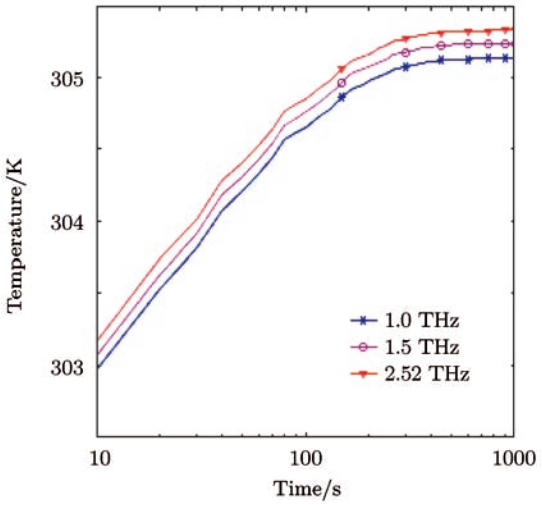


Fig. 9. Relationships between temperature and time for THz waves with different frequencies.

The contours in Fig. 10 show the process of temperature rising with time for the case of beam radius $a = 1$ mm. The temperature changes fast during the first 60 s and becomes constant after about 300 s. The highest temperature is at the centre of the incident surface.

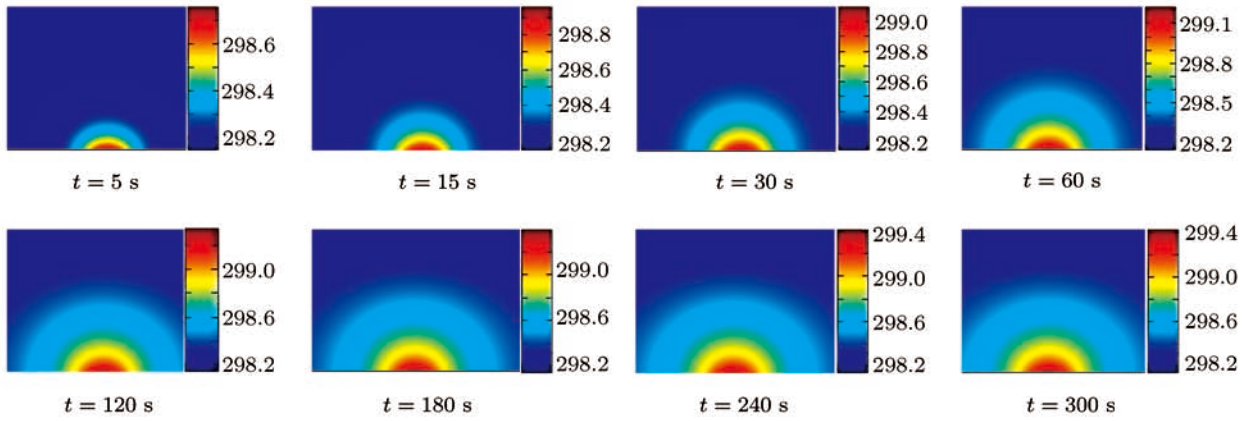


Fig. 10. Contours of temperature distribution versus time.

4. Conclusion

We report a simulation of transient temperature change on a static water layer exposed to a continuous THz wave. We learn that temperature takes about 300 s to reach a constant state under the conditions in our paper. The beam radius, the power and the frequency each have a small influence on the heating time, owing mainly to the thickness of the layer. The heating time depends mainly on the thickness of the layer. In this paper, we investigated the thermal effect on a relatively thin layer, which exists in many realistic cases but has not been studied yet. The beam has a Gaussian beam profile with a radius of 0.25 mm and can cause a maximum temperature increase of 7 K/mW. This work may motivate further study on the safe use of THz. For THz interaction with biotissue or other materials, there remain many questions to be answered.

References

[1] Hu B B and Nuss M C 1995 *Opt. Lett.* **20** 1716

[2] Pickwell E, Fitzgerald A J, Taday P F, Cole B E, Pye R J, Ha T, Pepper M and Wallace V P 2004 *Proceedings of the Joint 29th International Conference on Infrared and Millimeter Waves and 12th International Conference on Terahertz Electronics*, September 27–October 1, 2004, Karlsruhe, Germany, p. 821

[3] Kawase K, Ogawa Y and Watanabe Y 2003 *Opt. Express* **11** 2549

[4] Chen J, Chen Y Q, Zhao H W, Bastiaans G J and Zhang X C 2007 *Opt. Express* **15** 12060

[5] Piesiewicz R, Kleine-Ostmann T, Krumbholz N, Mittleman D, Koch M, Schoebel J and Kurner T 2007 *IEEE Antennas and Propagation Magazine* **49** 24

[6] Wang Y Y, Minamide H, Tang M, Notake T and Ito H 2010 *Opt. Express* **18** 15504

[7] Bondar N P, Kovalenko I L, Avgustinovich D F, Khamoyan A G and Kudryavtseva N N 2008 *Bull. Exp. Biol. Med.* **145** 401

[8] Alexandrov B S, Gelev V, Bishop A R, Usheva A and Rasmussen K Ø 2010 *Phys. Lett.* A **374** 1214

[9] Olshevskaya J S, Ratushnyak A S, Petrov A K, Kozlov A S and Zapara T A 2008 *Proceedings of the IEEE Region 8 International Conference on Computational Technologies in Electrical and Electronics Engineering*, July 21–25, 2008, Novosibirsk, Russia, p. 210

[10] Kristensen T T L, Withayachumnankul W, Jepsen P U and Abbott D 2010 *Opt. Express* **18** 4727

[11] Frauchiger J, Albers P and Weber H P 1992 *IEEE Journal of Quantum Electronics* **28** 1046

[12] Ellison W J 2007 *J. Phys. Chem. Ref. Data* **36** 1

[13] Ramires M L V, Nieto de Castro C A, Nagasaka Y, Nagashima A, Assael M J and Wakeham W A 1995 *J. Phys. Chem. Ref. Data* **24** 1377

[14] Xu J, Plaxco K W and Allen S J 2006 *J. Chem. Phys.* **124** 1